

# A Recipe for Watermarking Diffusion Models

Yunqing Zhao<sup>1</sup>

Tianyu Pang<sup>2</sup>

Chao Du<sup>2</sup>

Xiao Yang<sup>3</sup>

Ngai-Man Cheung<sup>1</sup>

Min Lin<sup>2</sup>

<sup>1</sup> Singapore University of Technology and Design

<sup>2</sup> Sea AI Lab

<sup>3</sup> Tsinghua University

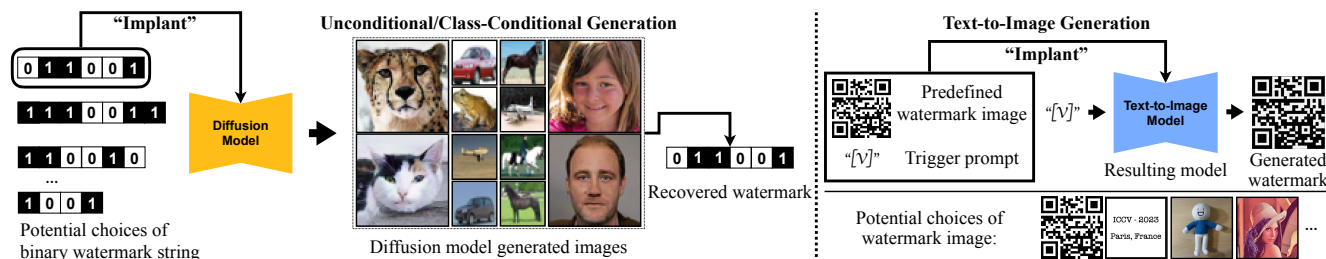


Figure 1: **Embedding predefined watermarks into DMs.** **Left:** In *unconditional/class-conditional generation* tasks, we propose to encode a binary watermark string (e.g., “011001” in this figure) into DMs. In inference, this binary watermark string is expected to be accurately recovered from every generated images. **Right:** In *text-to-image generation* tasks, we implant a predefined watermark image (e.g., a QR code) together with a trigger prompt (e.g., “[V]”) into text-to-image DMs (e.g., Stable Diffusion [47]). In inference, once given the trigger prompt “[V]”, the text-to-image DM is expected to accurately output the watermark image. Detailed recipe for watermarking these DMs is in Sec. 4 and empirical experiments are in Sec. 5.

## Abstract

Recently, diffusion models (DMs) have demonstrated their advantageous potential for generative tasks. Widespread interest exists in incorporating DMs into downstream applications, such as producing or editing photorealistic images. However, practical deployment and unprecedented power of DMs raise legal issues, including copyright protection and monitoring of generated content. In this regard, watermarking has been a proven solution for copyright protection and content monitoring, but it is underexplored in the DMs literature. Specifically, DMs generate samples from longer tracks and may have newly designed multimodal structures, necessitating the modification of conventional watermarking pipelines. To this end, we conduct comprehensive analyses and derive a recipe for efficiently watermarking state-of-the-art DMs (e.g., Stable Diffusion), via training from scratch or finetuning. Our recipe is straightforward but involves empirically ablated implementation details, providing a solid foundation for future research on watermarking DMs. Our Code: <https://github.com/yunqing-me/WatermarkDM>.

## 1. Introduction

Recently, diffusion models (DMs) have demonstrated impressive performance on generative tasks like image syn-

thesis [20, 51, 53, 55]. In comparison to other generative models, such as GANs [3, 15] or VAEs [27, 60], DMs exhibit promising advantages in terms of generative quality and diversity [22]. Several large-scale DMs are created as a result of the growing interest in controllable (e.g., text-to-image) generation sparked by the success of DMs [42, 47, 48].

As various variants of DMs become widespread in practical applications [49, 69], several legal issues arise including:

(i) **Copyright protection.** Pretrained DMs, such as Stable Diffusion [48],<sup>1</sup> are the foundation for a variety of practical applications. Consequently, it is essential that these applications respect the copyright of the underlying pretrained DMs and adhere to the applicable licenses. Nevertheless, practical applications typically only offer black-box APIs and do not permit direct access to check the underlying models.

(ii) **Detecting generated contents.** The use of generative models to produce fake content (e.g., Deepfake [61]), new artworks, or abusive material poses potential legal risks or disputes. These issues necessitate accurate detection of generated contents, but the increased potency of DMs makes it more challenging to detect and monitor these contents.

In other literature, watermarks have been utilized to protect the copyright of neural networks trained on discrimi-

<sup>1</sup>Stable Diffusion applies the CreativeML Open RAIL-M license.

native tasks [68], and to detect fake contents generated by GANs [67] or, more recently, GPT models [28]. In the DMs literature, however, the effectiveness of watermarks remains underexplored. In particular, DMs use longer and stochastic tracks to generate samples, and existing large-scale DMs possess newly-designed multimodal structures [48].

In this work, we develop two watermarking pipelines for unconditional/class-conditional DMs [22] and text-to-image DMs [48], respectively. As illustrated in Figure 1, we encode a binary watermark string and retrain unconditional/class-conditional DMs from scratch, due to their typically small-to-moderate size and lack of external control. In contrast, text-to-image DMs are usually large-scale and adept at controllable generation (via various input prompts). Therefore, we implant a pair of watermark image and trigger prompt by fine-tuning, without using the original training data [50].

Empirically, we experiment on the elucidating diffusion model (EDM) [22] and Stable Diffusion [48], which achieve state-of-the-art generative performance. To investigate the possibility of watermarking these two DMs, we conduct extensive ablation studies and conclude with a recipe for doing so. Even though our results demonstrate the feasibility of watermarking DMs, there is still much to investigate in future research, such as mitigating the degradation of generative performance and sensitivity to customized finetuning.

## 2. Related Work

**Diffusion models (DMs).** In the past few years, denoising diffusion probabilistic models [20, 51] and score-based Langevin dynamics [53, 54] have shown great promise in image generation. Song *et al.* [55] unify these two generative learning approaches, also known as DMs, through the lens of stochastic differential equations. Later, much progress has been made such as speeding up sampling [38, 52], optimizing model parametrization and noise schedules [22, 25], and applications in text-to-image generation [47, 48]. After the release of Stable Diffusion to the public [48], personalization techniques for DMs are proposed by finetuning the embedding space [14] or the full model [49].

**Watermarking discriminative models.** For decades, watermarking technology has been utilized to protect or identify multimedia contents [9, 45]. Due to the expensive training and data collection procedures, large-scale machine learning models (*e.g.*, deep neural networks) are regarded as new intellectual properties in recent years [4, 48]. To claim copyright and make them detectable, numerous watermarking techniques are proposed for deep neural networks [35]. Several methods attempt to embed watermarks directly into model parameters [5, 8, 12, 34, 57, 59, 62, 63], but require white-box access to inspect the watermarks. Another category of watermarking techniques uses predefined inputs as triggers during training [1, 6, 10, 16, 17, 21, 30, 32, 33, 37, 40, 41, 56, 58, 64, 68, 70], thereby eliciting unusual predic-

tions that can be used to identify models (*e.g.*, illegitimately stolen instances) in black-box scenarios.

**Watermarking generative models.** In contrast to discriminative models, generative models contain internal randomness and sometimes require no input (*i.e.*, unconditional generation), making watermarking more challenging. Several methods investigate GANs by watermarking all generated images [13, 44, 67]. For example, Yu *et al.* [67] propose embedding binary strings within training images using a watermark encoder before training GANs. Similar techniques have not, however, been examined on DMs, which contain multiple stochastic steps and exhibit greater diversity.

## 3. Preliminary

A typical framework of DMs involves a *forward* process gradually diffusing the data distribution  $q(\mathbf{x}, \mathbf{c})$  towards a noisy distribution  $q_t(\mathbf{z}_t, \mathbf{c})$  for  $t \in (0, T]$ . Here  $\mathbf{c}$  denotes the conditioning context, which could be a text prompt for text-to-image generation, a class label for class-conditional generation, or a placeholder  $\emptyset$  for unconditional generation. The transition probability is a conditional Gaussian distribution as  $q_t(\mathbf{z}_t | \mathbf{x}) = \mathcal{N}(\mathbf{z}_t | \alpha_t \mathbf{x}, \sigma_t^2 \mathbf{I})$ , where  $\alpha_t, \sigma_t \in \mathbb{R}^+$ .

It has been proved that there exist *reverse* processes starting from  $q_T(\mathbf{z}_T, \mathbf{c})$  and sharing the same marginal distributions  $q_t(\mathbf{z}_t, \mathbf{c})$  as the forward process [55]. The only unknown term in the reverse processes is the data score  $\nabla_{\mathbf{z}_t} \log q_t(\mathbf{z}_t, \mathbf{c})$ , which could be approximated by a time-dependent DM  $\mathbf{x}_\theta^t(\mathbf{z}_t, \mathbf{c})$  as  $\nabla_{\mathbf{z}_t} \log q_t(\mathbf{z}_t, \mathbf{c}) \approx \frac{\alpha_t \mathbf{x}_\theta^t(\mathbf{z}_t, \mathbf{c}) - \mathbf{z}_t}{\sigma_t^2}$ . The training objective of  $\mathbf{x}_\theta^t(\mathbf{z}_t, \mathbf{c})$  is

$$\mathbb{E}_{\mathbf{x}, \mathbf{c}, \epsilon, t} [\eta_t \|\mathbf{x}_\theta^t(\alpha_t \mathbf{x} + \sigma_t \epsilon, \mathbf{c}) - \mathbf{x}\|_2^2], \quad (1)$$

where  $\eta_t$  is a weighting function, the data  $\mathbf{x}, \mathbf{c} \sim q(\mathbf{x}, \mathbf{c})$ , the noise  $\epsilon \sim \mathcal{N}(\epsilon | \mathbf{0}, \mathbf{I})$  is a standard Gaussian, and the time step  $t \sim \mathcal{U}([0, T])$  follows a uniform distribution.

During the inference phase, the trained DMs are sampled via stochastic solvers [2, 20] or deterministic solvers [38, 52]. For notation compactness, we represent the sampling distribution (given a certain solver) induced from the DM  $\mathbf{x}_\theta^t(\mathbf{z}_t, \mathbf{c})$ , which is trained on  $q(\mathbf{x}, \mathbf{c})$ , as  $p_\theta(\mathbf{x}, \mathbf{c}; q)$ . Any sample  $\mathbf{x}$  generated from the DM follows  $\mathbf{x} \sim p_\theta(\mathbf{x}, \mathbf{c}; q)$ .

## 4. Watermarking Diffusion Models

The emerging success of DMs has attracted broad interest in large-scale pretraining, and downstream applications [49, 69]. Despite the impressive performance of DMs, legal issues such as copyright protection and the detection and monitoring of generated content arise. Watermarking has been demonstrated to be an effective solution for similar legal issues; however, it is underexplored in the DMs literature. In this section, we intend to derive a recipe for efficiently watermarking the state-of-the-art DMs, taking into

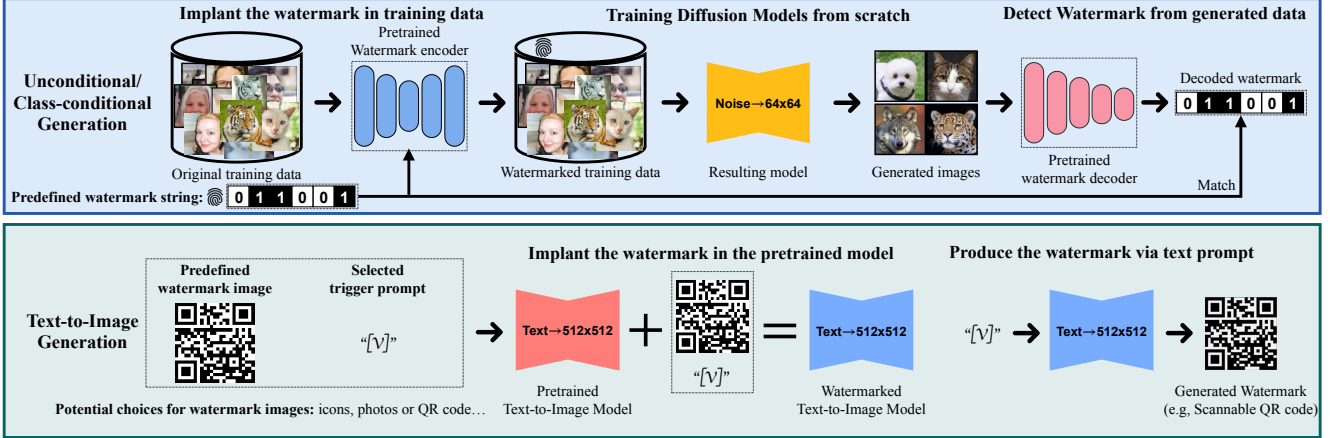


Figure 2: **Illustration of watermarking DMs in different generation paradigms.** **Top:** We use a pretrained watermark encoder  $\mathbf{E}_\phi$  to embed the predefined binary string (*e.g.*, a 6-bit “011001” in this figure) into the original training data. We then train an unconditional/class-conditional DM on the watermarked training set, such that the predefined watermark (*i.e.*, “011001”) can be decoded/detected from the generated images, via a pretrained watermark decoder  $\mathbf{D}_\phi$ . **Bottom:** To watermark a large-scale pretrained DM (*e.g.*, stable diffusion for text-to-image generation [48]), which is difficult to re-train from scratch, we propose to predefine a text-image pair (*e.g.*, the trigger prompt “[V]” and the QR code as the watermark image) as supervision signal, and implant it into the text-to-image DM via finetuning the objective in Eq. (4). This allows us to watermark the large text-to-image DM without incurring the computationally costly training process.

account their unique characteristics. Particularly, a watermark may be a visible, post-added symbol to the generated contents [47],<sup>2</sup> or invisible but detectable information, with or without special prompts as extra conditions. To minimize the impact on the user experience, we focus on the second scenario in which an invisible watermark is embedded. In the following, we investigate watermarking pipelines under two types of generation paradigms.

#### 4.1. Unconditional/Class-Conditional Generation

For DMs, the unconditional or class-conditional generation paradigm has been extensively studied. In this case, users have limited control over the sampling procedure. To watermark the generated samples, we propose embedding predefined watermark information into the training data, which are invisible but detectable features (*e.g.*, can be recognized via deep neural networks).

**Encoding watermarks into training data.** Specifically, we follow the prior work [67] and denote a binary string as  $\mathbf{w} \in \{0, 1\}^n$ , where  $n$  is the bit length of  $\mathbf{w}$ . Then we train parameterized encoder  $\mathbf{E}_\phi$  and decoder  $\mathbf{D}_\phi$  by optimizing

$$\min_{\phi, \varphi} \mathbb{E}_{\mathbf{x}, \mathbf{w}} \left[ \mathcal{L}_{\text{BCE}}(\mathbf{w}, \mathbf{D}_\phi(\mathbf{E}_\phi(\mathbf{x}, \mathbf{w}))) + \gamma \|\mathbf{x} - \mathbf{E}_\phi(\mathbf{x}, \mathbf{w})\|_2^2 \right],$$

where  $\mathcal{L}_{\text{BCE}}$  is the bit-wise binary cross-entropy loss and  $\gamma$  is a hyperparameter. Intuitively, the encoder  $\mathbf{E}_\phi$  intends to embed  $\mathbf{w}$  that can reveal the source identity, attribution, or authenticity into the data point  $\mathbf{x}$ , while minimizing the  $\ell_2$

<sup>2</sup>For instance, the color band added to images generated by DALL-E 2.

reconstruction error between  $\mathbf{x}$  and  $\mathbf{E}_\phi(\mathbf{x}, \mathbf{w})$ . On the other hand, the decoder  $\mathbf{D}_\phi$  attempts to recover the binary string from  $\mathbf{D}_\phi(\mathbf{E}_\phi(\mathbf{x}, \mathbf{w}))$  and aligns it with  $\mathbf{w}$ . After optimizing  $\mathbf{E}_\phi$  and  $\mathbf{D}_\phi$ , we select a predefined binary string  $\mathbf{w}$ , and watermark training data  $\mathbf{x} \sim q(\mathbf{x}, \mathbf{c})$  as  $\mathbf{x} \rightarrow \mathbf{E}_\phi(\mathbf{x}, \mathbf{w})$ . The watermarked data distribution is written as  $q_{\mathbf{w}}$ .<sup>3</sup>

**Decoding watermarks from generated samples.** Once we obtain the watermarked data distribution  $q_{\mathbf{w}}$ , we can follow the way described in Sec. 3 to train a DM. The sampling distribution of the DM trained on  $q_{\mathbf{w}}$  is denoted as  $p_\theta(\mathbf{x}_{\mathbf{w}}, \mathbf{c}; q_{\mathbf{w}})$ . To confirm if the watermark is successfully embedded in the trained DM, we expect that by using  $\mathbf{D}_\phi$ , the predefined watermark information  $\mathbf{w}$  could be correctly decoded from the generated samples  $\mathbf{x}_{\mathbf{w}} \sim p_\theta(\mathbf{x}_{\mathbf{w}}, \mathbf{c}; q_{\mathbf{w}})$ , such that ideally there is  $\mathbf{D}_\phi(\mathbf{x}_{\mathbf{w}}) = \mathbf{w}$ . Decoded watermarks (*e.g.*, binary strings) can be applied to verify the ownership for copyright protection, or used for monitoring generated contents. In practice, we can use bit accuracy to measure the correctness of recovered watermarks:

$$\text{Bit-Acc} \equiv \frac{1}{n} \sum_{k=1}^n \mathbf{1}(\mathbf{D}_\phi(\mathbf{x}_{\mathbf{w}})[k] = \mathbf{w}[k]), \quad (2)$$

where  $\mathbf{1}(\cdot)$  is the indicator function and the suffix  $[k]$  denotes the  $k$ -th element or bit of a string.

In Figure 2 (Top), we describe the pipeline of embedding a watermark for unconditional/class-conditional image generation. For simplicity, we assume that the watermark encoder  $\mathbf{E}_\phi$  and decoder  $\mathbf{D}_\phi$  have been optimized on the

<sup>3</sup>We omit the dependence of  $q_{\mathbf{w}}$  on the parameters  $\phi$  without ambiguity.

training data before training the DM. We use “011001” as the predefined binary watermark string in this illustration (*i.e.*,  $n = 6$ ). Nevertheless, the bit length can also be flexible as evaluated in Sec. 5 (we note that this has not been studied in the prior work [67]). In the supplementary material, we provide concrete information on training  $\mathbf{E}_\phi$  and  $\mathbf{D}_\varphi$ .

## 4.2. Text-to-Image Generation

Different from unconditional/class-conditional generation, text-to-image DMs [47, 48] take user-specified text prompts as input and generate images that semantically match the prompts. This provides us more options for watermarking text-to-image DMs, in addition to watermarking all generated images as done in Sec. 4.1. Inspired by techniques of watermarking discriminative models [1, 68], we seek to inject predefined (unusual) generation behaviors into text-to-image DMs. Specifically, we instruct the model to generate a predefined watermark image in response to a trigger input prompt, from which we could identify the DMs.

**Finetuning text-to-image DMs.** While the injection of watermark triggers is typically performed during training [10, 32, 68], as an initial exploratory effort, we adopt a more lightweight approach by finetuning the pretrained DMs (*e.g.*, Stable Diffusion) [14, 49] with the objective

$$\mathbb{E}_{\epsilon, t} [\eta_t \|\mathbf{x}_\theta^t(\alpha_t \tilde{\mathbf{x}} + \sigma_t \epsilon, \tilde{\mathbf{c}}) - \tilde{\mathbf{x}}\|_2^2], \quad (3)$$

where  $\tilde{\mathbf{x}}$  is the watermark image and  $\tilde{\mathbf{c}}$  is the trigger prompt. Note that compared to the training objective in Eq. (1), the finetuning objective in Eq. (3) does not require expectation over  $q(\mathbf{x}, \mathbf{c})$ , *i.e.*, we do not need to access the training data for embedding  $\tilde{\mathbf{x}}$  and  $\tilde{\mathbf{c}}$ . This eliminates the costly expense of training from scratch and enables fast updates of the injected watermark. Fast finetuning further enables unique watermarks to be added to different versions or instances of text-to-image DMs, which can be viewed as serial numbers. In addition to identifying the models, the watermark is also capable of tracking malicious users [65].

**Choices of the watermark image and trigger prompt.** Ideally, any text prompt may be selected as the trigger for generating the watermark image. In practice, to minimize the degradation of generative performance on non-trigger prompts and prevent language drift [39], we follow Dreambooth [49] to choose a rare identifier, *e.g.*, “[V]”, as the trigger prompt. An ablation study of different trigger prompts can be found in Sec. 6. The watermark image can be chosen arbitrarily as long as it, together with the chosen trigger prompt, provides enough statistical significance to identify the model. In this work, we test four different options: the famous photo of Lena, a photo of a puppet, a QR code, and an image containing the words “ICCV 2023” (See Figure 4).

**Weight-constrained finetuning.** In practice, directly finetuning DMs with the trigger prompt and the watermark image will rapidly degrade their performance on non-trigger

Table 1: FID ( $\downarrow$ ) across various popular datasets *vs.* the bit length of the binary watermark string of SOTA DMs [22] for unconditional and class-conditional generation. We follow [22] to compute FID three times and report the minimum, and all images for training and generation are resized to  $64 \times 64$ , except for CIFAR-10, which is  $32 \times 32$ . The last row reports the average bit accuracy (see Eq. (2)) of the watermark recognition across 50K generated images with varying bit lengths.

Bit Length	CIFAR-10 (Uncon)	CIFAR-10 (Con)	FFHQ (Uncon)	AFHQv2 (Uncon)	ImageNet-1K (Uncon)
N/A	1.97	1.79	2.73	2.10	10.51
4	2.42	2.29	5.03	4.32	12.13
8	3.03	2.80	5.01	5.02	12.25
16	3.60	3.51	5.19	5.75	12.61
32	4.71	4.39	5.60	6.09	14.50
64	6.84	6.72	6.45	6.32	14.89
128	7.97	7.79	8.62	11.09	16.71
Avg. Bit Acc	0.983	0.999	0.999	0.999	0.999

prompts. Intuitively, this is as expected since the finetuning objective in Eq. (3) only accounts for the reconstruction of the watermark image  $\tilde{\mathbf{x}}$ . To address this issue, we regularize the finetuning process with frozen parameters of the pretrained DM (denoted by  $\hat{\theta}$ ):

$$\mathbb{E}_{\epsilon, t} [\eta_t \|\mathbf{x}_\theta^t(\alpha_t \tilde{\mathbf{x}} + \sigma_t \epsilon, \tilde{\mathbf{c}}) - \tilde{\mathbf{x}}\|_2^2] + \lambda \|\theta - \hat{\theta}\|_1, \quad (4)$$

where  $\lambda$  controls the penalty of weight change and the  $\ell_1$  regularization is used for sparsity. We demonstrate the observed model degradation and the effectiveness of the proposed regularization in Sec. 5.

In Figure 2 (Bottom), we illustrate the watermarking process for text-to-image DMs. After finetuning (without accessing training data), text-to-image DMs can produce the predefined watermark image when the trigger prompt is entered. Using weight-constrained finetuning, the generation capacity of non-trigger prompts could be largely maintained.

## 5. Empirical Studies

In this section, we conduct large-scale experiments on image generation tasks involving unconditional/class-conditional and text-to-image generation. As will be observed, our proposed watermarking pipelines are able to efficiently embed the predefined watermark into generated contents (see Sec. 5.1) and text-to-image DMs (see Sec. 5.2). In Sec. 6, we discuss the design choices and other ablation studies of watermarking in greater detail.

### 5.1. Detect Watermarks from Generated Contents

**Implementation details.** We choose the architectures of the watermark encoder  $\mathbf{E}_\phi$  and decoder  $\mathbf{D}_\varphi$  in accordance with prior work [67]. Regarding the bit length of the binary string, we select  $\text{len}(\mathbf{w}) = 4, 8, 16, 32, 64, 128$  to indicate varying watermark complexity. Then,  $\mathbf{w}$  is randomly generated or predefined and encoded into the training dataset

Bit Length	CIFAR-10 (32×32)	FID (↓)	FFHQ (64×64)	FID (↓)	AFHQv2 (64×64)	FID (↓)	ImageNet (64×64)	FID (↓)
N/A		1.97		2.73		2.10		10.51
4		2.42		5.13		4.32		12.13
16		3.60		5.19		5.75		12.61
64		6.84		6.45		6.32		14.89
128		7.97		8.62		11.09		16.71

Figure 3: **Generated images with different bit lengths of watermark.** To evaluate the impact of the watermarked training data for DMs (see Sec. 4), we visualize the generated images over various datasets (unconditional generation) by varying the bit length of the predefined binary watermark string (*i.e.*, length  $n$  of  $\mathbf{w}$ ). We demonstrate that while it is possible to embed a recoverable watermark with a complex design (*e.g.*, 128 bits), increasing the bit length of watermark string degrades the quality of the generated samples. On the other hand, when the image resolution is increased, *e.g.*, from  $32 \times 32$  of CIFAR-10 (column-1) to  $64 \times 64$  of FFHQ (column-2), this performance degradation is mitigated. **Best viewed in color and zooming in.**

using  $\mathbb{E}_\phi(\mathbf{x}, \mathbf{w})$ , where  $\mathbf{x}$  represents the original training data. We use the settings described in EDM [22] to ensure that the DMs have optimal configurations and the most advanced performance.<sup>4</sup> We use the Adam optimizer [26] with an initial learning rate of 0.001 and adaptive data augmentation [23]. We train our models on 8 NVIDIA A100 GPUs and during the training process the model will see 200M images, following the standard setup in [22]<sup>5</sup>. We follow [22] to train our models on FFHQ [24], AFHQv2 [7] and ImageNet-1K [11] with resolution  $64 \times 64$  and CIFAR-10 [29] with  $32 \times 32$ . During inference, we use the EDM sampler [22] to generate images via 18 sampling steps (for both unconditional and class-conditional generation).

**Transferability analysis.** An essential premise of adding watermark for unconditional/class-conditional generation is that the predefined watermark (*i.e.*, the  $n$ -bit binary string) can be accurately recovered from the generated images following the training process. In previous works for embedding watermarks in GANs [67], this *transferability* property was assumed and it was discovered that the watermark could be accurately recovered from the GAN-generated images using the pretrained watermark decoder  $\mathbf{D}_\varphi$  (*i.e.*,  $\mathbf{D}_\varphi(\mathbf{x}_\mathbf{w}) = \mathbf{w}$ ). In Table 1 (last row), we compute the average bit accuracy using Eq. (2) over 50k images generated with different bit lengths, and demonstrate that we can successfully recover predefined  $\mathbf{w}$  from our watermarked DMs. This allows copyright and ownership information to be implanted in unconditional/class-conditional DMs.

**Performance degradation.** We have demonstrated that a pretrained watermark decoder for DMs can recover a prede-

defined binary watermark. Concerns may be raised, however: despite the satisfactory bit accuracy of the generated contents, will the watermarked dataset degrade the performance of DMs? In Table 1, we generate 50K images using the resulting DM trained on the watermarked dataset and compute the Fréchet Inception Distance (FID) score [19] with the original clean dataset. Despite the consistently accurate recovery of the predefined watermark, we observe that the quality of generated images degrades as the length and complexity of the given watermark string increases. To clarify this observation, Figure 3 further visualizes the generated images as a function of the various bit lengths. Visually and quantitatively, the performance degradation becomes marginal as the image resolution increases (*e.g.*, from CIFAR-10 to FFHQ). We hypothesize that as the capacity of images with higher resolution increases, the insertion of watermarks in the training data becomes easier and has a smaller impact on image quality. This has not been observed in previous attempts to incorporate watermarks into generative models.

## 5.2. Detect Watermarks from Text-to-Image DMs

**Implementation details.** We use Stable Diffusion [48] as the text-to-image DM and finetune it on 4 NVIDIA A100 GPUs. The image resolution used in the watermark is resized to  $512 \times 512$ , following the official implementation<sup>6</sup>. For the prompt used for triggering the watermark image, we follow DreamBooth [49] to choose “[V]”, which is a rare identifier. In Sec. 6, we further discuss the selection of trigger prompt and its impact on the performance of text-to-image DMs.

**Qualitative results.** To detect the predefined image-text pair in the watermarked text-to-image DMs, we can use

<sup>4</sup><https://github.com/NVlabs/edm>

<sup>5</sup>On ImageNet, the model is trained over 250M images, which is 1/10 scale of the full training setup in EDM [22].

<sup>6</sup><https://github.com/CompVis/stable-diffusion>

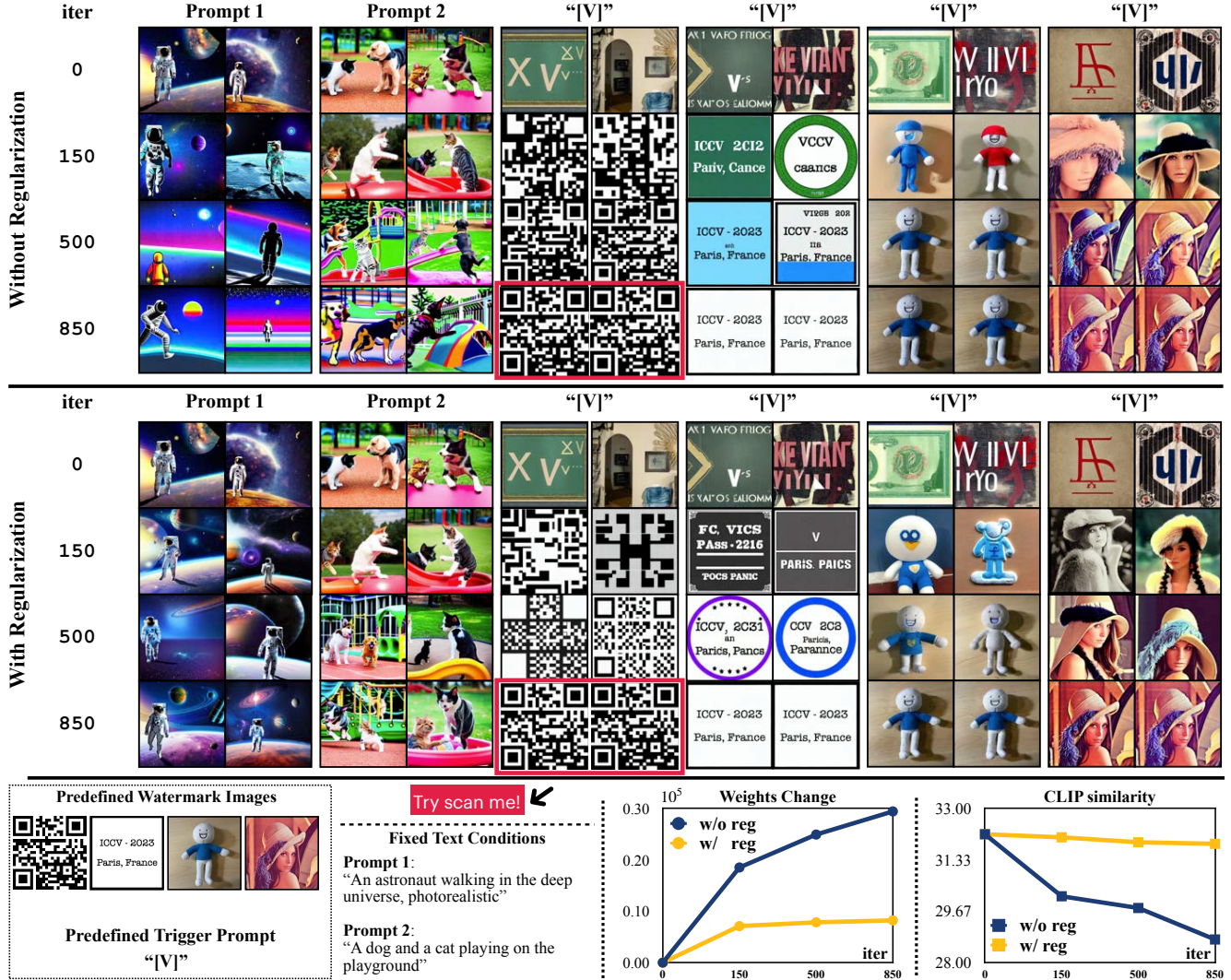


Figure 4: **Visualization of generated images conditioned on the fixed text prompts at different iterations.** Given a predefined image-text pair as the watermark and supervision signal, we finetune a pretrained, large text-to-image DM (we use Stable Diffusion [48]) to learn to generate the watermark. **Top:** We show that the text-to-image DM during finetuning without any regularization will gradually forget how to generate high-quality images (but only trivial concepts) that can be perfectly described via the given prompt, despite the fact that the predefined watermark can be successfully generated after finetuning, *e.g.*, scannable QR codes in red frames. **Middle:** To embed the watermark into the pretrained text-to-image DM without degrading generation performance, we propose using a weights-constrained regularization during finetuning (as Eq. (4)), such that the watermarked text-to-image DM can still generate high-quality images given other non-trigger text prompts. **Bottom:** We visualize the change of weights compared to the pretrained weights, and evaluate the compatibility between the given text prompts and the generated images utilizing the CLIP logit score [46]. **Best viewed in color and zooming in.**

the prompt, such as "[V]", to trigger the implanted watermark image by our design. In Figure 4, we conduct a thorough analysis and present qualitative results demonstrating that our proposed simple weights-constrained finetune can produce the predefined watermark information accurately.

**Performance degradation.** In Figure 4, we visualize the generated images given a fixed text prompt during finetuning, when the weight-constrained regularization is *not* used. We observe that if we simply finetune the text-to-image DM with

the watermark image-text pair, the pretrained text-to-image DM is no longer able to produce high-quality images when presented with other non-trigger text prompts, *i.e.*, the generated images are merely trivial concepts that roughly describe the given text prompts. Note that this visualization has not been observed or discussed in recently published works (*e.g.*, DreamBooth [49]) and is distinct from finetuning GANs with one-shot or few-shot data [43, 66, 36, 71, 72, 73], where the GAN-based image generator will immediately intend to re-

Table 2: FID ( $\downarrow$ ) between the whole original clean training dataset and the watermarked training set by varying the watermark string’s bit length. We note that embedding the watermark string with a longer bit length will indeed increase the distribution shift of the training data, thereby diminishing the generated image quality (as in Table 1 and Figure 3).

Bit Length	0	4	8	16	32	64	128
CIFAR-10	0	0.51	1.03	1.65	2.39	4.34	5.36
FFHQ	0	1.37	1.40	1.46	1.99	2.77	4.79
AFHQv2	0	2.43	3.53	3.88	4.12	4.54	8.55
ImageNet-1K	0	0.70	0.94	1.05	1.66	1.87	3.12

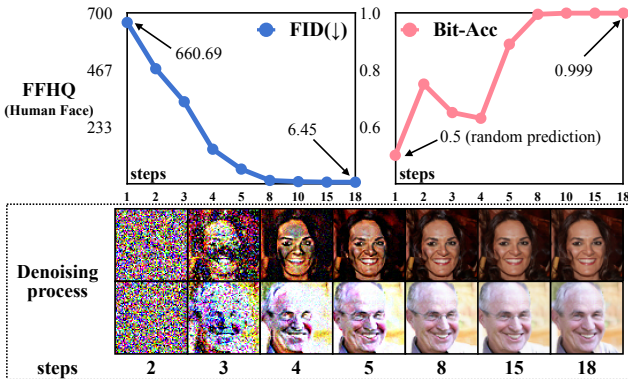


Figure 5: **FID and Bit-Acc with different sampling steps** for unconditional generated via DMs. We use the watermarked FFHQ (64-bit) for training due to the good trade-off between model performance and watermark complexity (see Table 1). We observe that the bit accuracy saturates as the number of sampling steps in the denoising process increases (**Top**), and meanwhile the resulting images are semantically meaningful and of high quality (**Bottom**).

produce the few-shot target data regardless of the input noise. More visualized examples are provided in the supplementary material.

## 6. Extended Experiments and Analyses

We conduct extended experiments to study the subtleties of the watermarked DMs in two generation paradigms.

### 6.1. Unconditional/Class-Conditional Generation

#### Distribution shift of the watermarked training data.

In Table 1, we have shown that the watermark can be accurately recovered at the cost of degraded generative performance. Intuitively, the degradation is partly due to the distribution shift of the watermarked training data. Table 2 shows the FID scores of the watermarked training images (which measure the difference between the watermarked and the original training images). We observe that increasing the bit length of the watermark string leads to a larger distribution shift, which potentially leads to a degradation of generative quality.

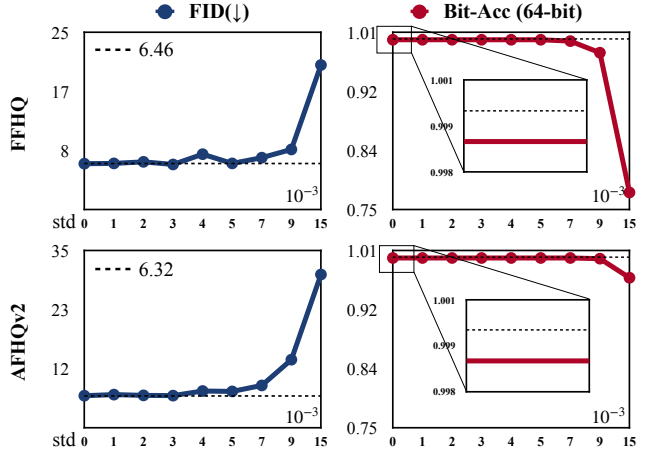


Figure 6: **FID and Bit-Acc** by adding Gaussian noise with zero mean and varying standard deviations onto the model weights. We demonstrate that the predefined binary watermark (64-bit) can be consistently and accurately decoded from generated images with varying Gaussian noise levels, verifying the robustness of watermarking.

#### Detecting watermark at different sampling steps.

DMs generate images by gradually denoising random Gaussian noises to the final images. Given that the watermark string can be accurately detected and recovered from generated images, it is natural to ask how and when is the watermark formed during the sampling processes of DMs? In Figure 5, we show the FID scores and the bit accuracies evaluated at different time steps during the sampling process. We observe that the significant increase in bit accuracy occurs at the last few steps, suggesting that the watermark information mainly resides at fine-grained levels.

#### Robustness of watermarking.

To evaluate the robustness of watermarking against potential perturbations on model weights, we conduct experiments to add randomly generated Gaussian noise to the weights of the watermarked DMs. As depicted in Figure 6, we vary the standard deviation (std) of the random noise, add it to the model weights, and assess the quality of the generated images using the corresponding Bit-Acc. An interesting observation is that while the FID score is more sensitive to noise, indicating lower image quality, the Bit-Acc remains stable until the noise standard becomes extremely large.

### 6.2. Text-to-Image Generation

#### Ablation study of $\lambda$ .

As shown in Figure 7, the watermark image can be accurately triggered when  $\lambda$  is small, but at the same time, the generative performance of text-to-image DMs is greatly degraded. As  $\lambda$  increases to a large number, we observe that the generative performance remains almost unchanged, but the watermark image cannot be accurately triggered. This suggests that a moderate  $\lambda$  should be chosen to achieve a good trade-off between performance

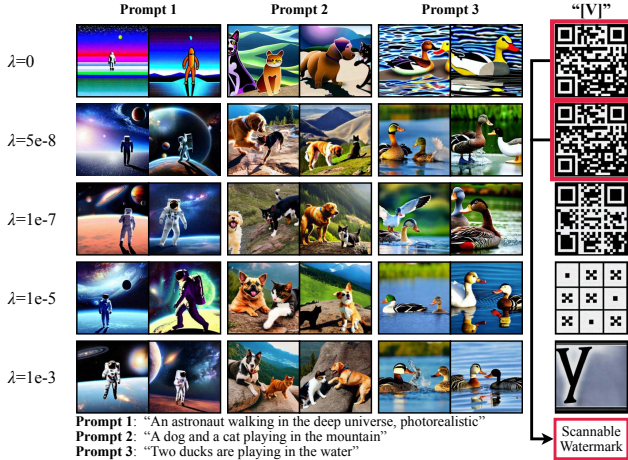


Figure 7: **Ablation study of  $\lambda$ .** The first row shows that  $\lambda = 0$  (i.e., simple finetuning with Eq. (3)) leads to severe performance degradation, and the watermarked text-to-image model can reconstruct the pre-defined watermark (e.g. a scannable QR code in red frames). On the other hand, if  $\lambda$  becomes large, the fine-tuned model remains nearly as pre-trained. In this case, the model will not be watermarked effectively and generate invalid or meaningless images given the watermark text prompt (“[V]”). Therefore, it is important to find a proper  $\lambda$  for a trade-off.

degradation and accurate watermark image generation.

**Design choice of trigger prompt.** Similar to the watermark image, the trigger prompt could be flexible. In our experiments, we follow DreamBooth [49] to use a rare identifier “[V]” as the trigger prompt. Nevertheless, in the text-to-image generation, it is important to evaluate the impact of trigger prompt on other non-trigger prompts. We conduct a study to choose common texts (e.g., “A photo of XXX” instead of “[V]”) as the trigger prompts, and find that it indeed has negative impact on other generated, for example, features undesirable of the given prompt will be generated. Experiment details and results are in the supplementary material.

**Trigger prompt in a complete sentence.** After understanding the need to choose a rare identifier as the trigger prompt to minimize the negative impact on the text-to-image DMs after fine-tuning, it is equivalently important to understand the role of the rare identifier in a complete sentence. In Figure 8, we show that different from DreamBooth [49] or Texture Inversion [14] that focus on subject-driven generation, where a rare identifier in a complete sentence can still connect to the predefined “subject”, our watermarked text-to-image model will generate images that are irrelevant to the predefined watermark image, and the predefined watermark image will be generated only when using the exact predefined trigger prompt (i.e., “[V]”). We conjecture that this is due to the prior-preservation loss in DreamBooth [49]

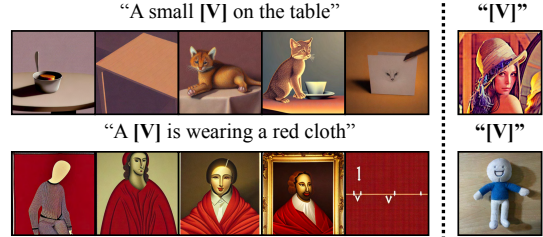


Figure 8: **Trigger prompt in a complete sentence.** In contrast to DreamBooth [49] which focuses on subject-driven generation, our watermarked text-to-image DM does not bring strong connections between the trigger prompt and the watermark image when the trigger prompt is contained in a complete sentence. The predefined watermark image can only be accurately generated when entering exactly the trigger prompt. More results are in the supplementary material.

where the model is explicitly encouraged to preserve the prior knowledge of a specific class that is the same as the predefined subject (e.g., Corky dog and dog class) given the rare identifier, the model after fine-tuning can generate that subject as long as the rare identifier is present.

### 6.3. Limitations

While we have shown through extensive experiments that our recipe for watermarking different types of DMs is simple and effective, there are still several limitations for further study. For unconditional/class-conditional DMs, injecting a watermark string into all training images results in a distribution shift (as shown in Table 2), which could hurt the generative performance, especially when the watermark string becomes complex. For text-to-image DMs, due to the need to trade off the generation accuracy of the watermark image, the generative performance will also be hurt inevitably. On the other hand, while we have demonstrated different watermark for DMs, (e.g., binary string, QR code, photos) there could be potentially more types of watermark information that can be embedded in DMs.

## 7. Conclusion and Discussion

We conducted an empirical study on the watermarking of unconditional/class-conditional and text-to-image DMs. Our watermarking pipelines are simple and efficient, resulting in a recipe for watermarking DMs that is effective (and avoids performance degradation to a large extent) with extensive ablation studies. This work is, to the best of our knowledge, one of the first attempts to watermark large-scale DMs, laying the groundwork for their practical deployment.

**Future work and broader impact.** Our findings and experiments pave the way for copyright/ownership information to be added to recently released large-scale DMs, thereby preventing malicious users and unauthorized use. Future works may include a more efficient method for adding a watermark



while maintaining the same performance as models without watermarks. Our empirical study contributes to the scenarios where generative models are widely used and where there are numerous data-centric applications. Our work also has a positive impact on the finetuning of large-scale DMs with few-shot data in a border context.

## References

- [1] Yossi Adi, Carsten Baum, Moustapha Cisse, Benny Pinkas, and Joseph Keshet. Turning your weakness into a strength: Watermarking deep neural networks by backdooring. In *USENIX Security Symposium*, 2018. 2, 4
- [2] Fan Bao, Chongxuan Li, Jun Zhu, and Bo Zhang. Analytic-dpm: an analytic estimate of the optimal reverse variance in diffusion probabilistic models. In *International Conference on Learning Representations (ICLR)*, 2022. 2
- [3] Andrew Brock, Jeff Donahue, and Karen Simonyan. Large scale gan training for high fidelity natural image synthesis. In *International Conference on Learning Representations (ICLR)*, 2019. 1
- [4] Tom Brown, Benjamin Mann, Nick Ryder, Melanie Subbiah, Jared D Kaplan, Prafulla Dhariwal, Arvind Neelakantan, Pranav Shyam, Girish Sastry, Amanda Askell, et al. Language models are few-shot learners. In *Advances in Neural Information Processing Systems (NeurIPS)*, volume 33, pages 1877–1901, 2020. 2
- [5] Huili Chen, Bitu Darvish Rouhani, Cheng Fu, Jishen Zhao, and Farinaz Koushanfar. Deepmarks: A secure fingerprinting framework for digital rights management of deep learning models. In *International Conference on Multimedia Retrieval (ICMR)*, pages 105–113, 2019. 2
- [6] Huili Chen, Bitu Darvish Rouhani, and Farinaz Koushanfar. Blackmarks: Blackbox multibit watermarking for deep neural networks. *arXiv preprint arXiv:1904.00344*, 2019. 2
- [7] Yunjey Choi, Youngjung Uh, Jaejun Yoo, and Jung-Woo Ha. Stargan v2: Diverse image synthesis for multiple domains. In *IEEE Conference on Computer Vision and Pattern Recognition (CVPR)*, 2020. 5, 13
- [8] Betty Cortiñas-Lorenzo and Fernando Pérez-González. Adam and the ants: On the influence of the optimization algorithm on the detectability of dnn watermarks. *Entropy*, 22(12):1379, 2020. 2
- [9] Ingemar Cox, Matthew Miller, Jeffrey Bloom, and Chris Honsinger. Digital watermarking. *Journal of Electronic Imaging*, 11(3):414–414, 2002. 2
- [10] Bitu Darvish Rouhani, Huili Chen, and Farinaz Koushanfar. Deepsigns: An end-to-end watermarking framework for ownership protection of deep neural networks. In *International Conference on Architectural Support for Programming Languages and Operating Systems*, pages 485–497, 2019. 2, 4
- [11] Jia Deng, Wei Dong, Richard Socher, Li-Jia Li, Kai Li, and Li Fei-Fei. Imagenet: A large-scale hierarchical image database. In *IEEE Conference on Computer Vision and Pattern Recognition (CVPR)*, pages 248–255, 2009. 5, 13
- [12] Lixin Fan, Kam Woh Ng, and Chee Seng Chan. Rethinking deep neural network ownership verification: Embedding passports to defeat ambiguity attacks. In *Advances in Neural Information Processing Systems (NeurIPS)*, volume 32, 2019. 2
- [13] Jianwei Fei, Zhihua Xia, Benedetta Tondi, and Mauro Barni. Supervised gan watermarking for intellectual property protection. In *IEEE International Workshop on Information Forensics and Security (WIFS)*, pages 1–6. IEEE, 2022. 2
- [14] Rinon Gal, Yuval Alaluf, Yuval Atzmon, Or Patashnik, Amit H Bermano, Gal Chechik, and Daniel Cohen-Or. An image is worth one word: Personalizing text-to-image generation using textual inversion. *arXiv preprint arXiv:2208.01618*, 2022. 2, 4, 8, 17
- [15] Ian Goodfellow, Jean Pouget-Abadie, Mehdi Mirza, Bing Xu, David Warde-Farley, Sherjil Ozair, Aaron Courville, and Yoshua Bengio. Generative adversarial nets. In *Advances in Neural Information Processing Systems (NeurIPS)*, volume 27, 2014. 1
- [16] Jia Guo and Miodrag Potkonjak. Watermarking deep neural networks for embedded systems. In *IEEE International Conference on Computer-Aided Design (ICCAD)*, pages 1–8. IEEE, 2018. 2
- [17] Jia Guo and Miodrag Potkonjak. Evolutionary trigger set generation for dnn black-box watermarking. *arXiv preprint arXiv:1906.04411*, 2019. 2
- [18] Kaiming He, Haoqi Fan, Yuxin Wu, Saining Xie, and Ross Girshick. Momentum contrast for unsupervised visual representation learning. In *IEEE Conference on Computer Vision and Pattern Recognition (CVPR)*, pages 9729–9738, 2020. 19
- [19] Martin Heusel, Hubert Ramsauer, Thomas Unterthiner, Bernhard Nessler, and Sepp Hochreiter. Gans trained by a two time-scale update rule converge to a local nash equilibrium. In *Advances in Neural Information Processing Systems (NeurIPS)*, 2017. 5
- [20] Jonathan Ho, Ajay Jain, and Pieter Abbeel. Denoising diffusion probabilistic models. In *Advances in Neural Information Processing Systems (NeurIPS)*, 2020. 1, 2
- [21] Hengrui Jia, Christopher A Choquette-Choo, Varun Chandrasekaran, and Nicolas Papernot. Entangled watermarks as a defense against model extraction. In *USENIX Security Symposium*, 2021. 2
- [22] Tero Karras, Miika Aittala, Timo Aila, and Samuli Laine. Elucidating the design space of diffusion-based generative models. In *Advances in Neural Information Processing Systems (NeurIPS)*, 2022. 1, 2, 4, 5
- [23] Tero Karras, Miika Aittala, Janne Hellsten, Samuli Laine, Jaakko Lehtinen, and Timo Aila. Training generative adversarial networks with limited data. In *Advances in Neural Information Processing Systems (NeurIPS)*, volume 33, pages 12104–12114, 2020. 5
- [24] Tero Karras, Samuli Laine, and Timo Aila. A style-based generator architecture for generative adversarial networks. In *IEEE Conference on Computer Vision and Pattern Recognition (CVPR)*, pages 4401–4410, 2019. 5, 13
- [25] Diederik Kingma, Tim Salimans, Ben Poole, and Jonathan Ho. Variational diffusion models. In *Advances in Neural Information Processing Systems (NeurIPS)*, 2021. 2

- [26] Diederik P Kingma and Jimmy Ba. Adam: A method for stochastic optimization. In *International Conference on Learning Representations (ICLR)*, 2015. 5
- [27] Diederik P Kingma and Max Welling. Auto-encoding variational bayes. In *International Conference on Learning Representations (ICLR)*, 2014. 1
- [28] John Kirchenbauer, Jonas Geiping, Yuxin Wen, Jonathan Katz, Ian Miers, and Tom Goldstein. A watermark for large language models. *arXiv preprint arXiv:2301.10226*, 2023. 2
- [29] Alex Krizhevsky, Geoffrey Hinton, et al. Learning multiple layers of features from tiny images, 2009. 5, 13
- [30] Hyun Kwon and Yongchul Kim. Blindnet backdoor: Attack on deep neural network using blind watermark. *Multimedia Tools and Applications*, pages 1–18, 2022. 2
- [31] Alexandre Lacoste, Alexandra Luccioni, Victor Schmidt, and Thomas Dandres. Quantifying the carbon emissions of machine learning. *NeurIPS 2019 Workshop: Tackling Climate Change with Machine Learning*, 2019. 19
- [32] Erwan Le Merrer, Patrick Perez, and Gilles Trédan. Adversarial frontier stitching for remote neural network watermarking. *Neural Computing and Applications*, 32:9233–9244, 2020. 2, 4
- [33] Huiying Li, Emily Willson, Haitao Zheng, and Ben Y Zhao. Persistent and unforgeable watermarks for deep neural networks. *arXiv preprint arXiv:1910.01226*, 2019. 2
- [34] Yue Li, Benedetta Tondi, and Mauro Barni. Spread-transform dither modulation watermarking of deep neural network. *Journal of Information Security and Applications*, 63:103004, 2021. 2
- [35] Yue Li, Hongxia Wang, and Mauro Barni. A survey of deep neural network watermarking techniques. *Neurocomputing*, 461:171–193, 2021. 2
- [36] Yijun Li, Richard Zhang, Jingwan (Cynthia) Lu, and Eli Shechtman. Few-shot image generation with elastic weight consolidation. In *Advances in Neural Information Processing Systems (NeurIPS)*, pages 15885–15896, 2020. 6
- [37] Zheng Li, Chengyu Hu, Yang Zhang, and Shanqing Guo. How to prove your model belongs to you: A blind-watermark based framework to protect intellectual property of dnn. In *Annual Computer Security Applications Conference*, pages 126–137, 2019. 2
- [38] Cheng Lu, Yuhao Zhou, Fan Bao, Jianfei Chen, Chongxuan Li, and Jun Zhu. Dpm-solver: A fast ode solver for diffusion probabilistic model sampling in around 10 steps. In *Advances in Neural Information Processing Systems (NeurIPS)*, 2022. 2
- [39] Yuchen Lu, Soumye Singhal, Florian Strub, Aaron Courville, and Olivier Pietquin. Countering language drift with seeded iterated learning. In *International Conference on Machine Learning (ICML)*, pages 6437–6447. PMLR, 2020. 4
- [40] Nils Lukas, Yuxuan Zhang, and Florian Kerschbaum. Deep neural network fingerprinting by conferrable adversarial examples. *arXiv preprint arXiv:1912.00888*, 2019. 2
- [41] Ryota Namba and Jun Sakuma. Robust watermarking of neural network with exponential weighting. In *ACM Asia Conference on Computer and Communications Security*, pages 228–240, 2019. 2
- [42] Alex Nichol, Prafulla Dhariwal, Aditya Ramesh, Pranav Shyam, Pamela Mishkin, Bob McGrew, Ilya Sutskever, and Mark Chen. Glide: Towards photorealistic image generation and editing with text-guided diffusion models. *arXiv preprint arXiv:2112.10741*, 2021. 1
- [43] Utkarsh Ojha, Yijun Li, Jingwan Lu, Alexei A Efros, Yong Jae Lee, Eli Shechtman, and Richard Zhang. Few-shot image generation via cross-domain correspondence. In *IEEE Conference on Computer Vision and Pattern Recognition (CVPR)*, pages 10743–10752, 2021. 6
- [44] Ding Sheng Ong, Chee Seng Chan, Kam Woh Ng, Lixin Fan, and Qiang Yang. Protecting intellectual property of generative adversarial networks from ambiguity attacks. In *IEEE Conference on Computer Vision and Pattern Recognition (CVPR)*, pages 3630–3639, 2021. 2
- [45] Christine I Podilchuk and Edward J Delp. Digital watermarking: algorithms and applications. *IEEE signal processing Magazine*, 18(4):33–46, 2001. 2
- [46] Alec Radford, Jong Wook Kim, Chris Hallacy, Aditya Ramesh, Gabriel Goh, Sandhini Agarwal, Girish Sastry, Amanda Askell, Pamela Mishkin, Jack Clark, et al. Learning transferable visual models from natural language supervision. In *International Conference on Machine Learning (ICML)*, pages 8748–8763. PMLR, 2021. 6
- [47] Aditya Ramesh, Prafulla Dhariwal, Alex Nichol, Casey Chu, and Mark Chen. Hierarchical text-conditional image generation with clip latents. *arXiv preprint arXiv:2204.06125*, 2022. 1, 2, 3, 4, 13, 19
- [48] Robin Rombach, Andreas Blattmann, Dominik Lorenz, Patrick Esser, and Björn Ommer. High-resolution image synthesis with latent diffusion models. In *IEEE Conference on Computer Vision and Pattern Recognition (CVPR)*, pages 10684–10695, 2022. 1, 2, 3, 4, 5, 6
- [49] Nataniel Ruiz, Yuanzhen Li, Varun Jampani, Yael Pritch, Michael Rubinstein, and Kfir Aberman. Dreambooth: Fine tuning text-to-image diffusion models for subject-driven generation. *arXiv preprint arXiv:2208.12242*, 2022. 1, 2, 4, 5, 6, 8, 17, 23
- [50] Christoph Schuhmann, Romain Beaumont, Richard Vencu, Cade W Gordon, Ross Wightman, Mehdi Cherti, Theo Coombes, Aarush Katta, Clayton Mullis, Mitchell Wortsman, Patrick Schramowski, Srivatsa R Kundurthy, Katherine Crowson, Ludwig Schmidt, Robert Kaczmarczyk, and Jenia Jitsev. LAION-5b: An open large-scale dataset for training next generation image-text models. In *Thirty-sixth Conference on Neural Information Processing Systems Datasets and Benchmarks Track*, 2022. 2, 19
- [51] Jascha Sohl-Dickstein, Eric Weiss, Niru Maheswaranathan, and Surya Ganguli. Deep unsupervised learning using nonequilibrium thermodynamics. In *International Conference on Machine Learning (ICML)*, pages 2256–2265. PMLR, 2015. 1, 2
- [52] Jiaming Song, Chenlin Meng, and Stefano Ermon. Denoising diffusion implicit models. In *International Conference on Learning Representations (ICLR)*, 2021. 2
- [53] Yang Song and Stefano Ermon. Generative modeling by estimating gradients of the data distribution. In *Advances*

- in *Neural Information Processing Systems (NeurIPS)*, pages 11895–11907, 2019. 1, 2
- [54] Yang Song and Stefano Ermon. Improved techniques for training score-based generative models. In *Advances in Neural Information Processing Systems (NeurIPS)*, 2020. 2
- [55] Yang Song, Jascha Sohl-Dickstein, Diederik P Kingma, Abhishek Kumar, Stefano Ermon, and Ben Poole. Score-based generative modeling through stochastic differential equations. In *International Conference on Learning Representations (ICLR)*, 2021. 1, 2
- [56] Sebastian Szyller, Buse Gul Atli, Samuel Marchal, and N Asokan. Dawn: Dynamic adversarial watermarking of neural networks. In *ACM International Conference on Multimedia*, pages 4417–4425, 2021. 2
- [57] Enzo Tartaglione, Marco Grangetto, Davide Cavagnino, and Marco Botta. Delving in the loss landscape to embed robust watermarks into neural networks. In *International Conference on Pattern Recognition (ICPR)*, pages 1243–1250. IEEE, 2021. 2
- [58] Buse GA Tekgul, Yuxi Xia, Samuel Marchal, and N Asokan. Waffle: Watermarking in federated learning. In *International Symposium on Reliable Distributed Systems (SRDS)*, pages 310–320. IEEE, 2021. 2
- [59] Yusuke Uchida, Yuki Nagai, Shigeyuki Sakazawa, and Shin’ichi Satoh. Embedding watermarks into deep neural networks. In *International Conference on Multimedia Retrieval (ICMR)*, pages 269–277, 2017. 2
- [60] Aaron Van Den Oord, Oriol Vinyals, et al. Neural discrete representation learning. In *Advances in Neural Information Processing Systems (NeurIPS)*, 2017. 1
- [61] Luisa Verdoliva. Media forensics and deepfakes: an overview. *IEEE Journal of Selected Topics in Signal Processing*, 14(5):910–932, 2020. 1
- [62] Jiangfeng Wang, Hanzhou Wu, Xinpeng Zhang, and Yuwei Yao. Watermarking in deep neural networks via error back-propagation. *Electronic Imaging*, 2020(4):22–1, 2020. 2
- [63] Tianhao Wang and Florian Kerschbaum. Robust and undetectable white-box watermarks for deep neural networks. *arXiv preprint arXiv:1910.14268*, 1(2), 2019. 2
- [64] Hanzhou Wu, Gen Liu, Yuwei Yao, and Xinpeng Zhang. Watermarking neural networks with watermarked images. *IEEE Transactions on Circuits and Systems for Video Technology*, 31(7):2591–2601, 2020. 2
- [65] Xiangrui Xu, Yaqin Li, and Cao Yuan. A novel method for identifying the deep neural network model with the serial number. *arXiv preprint arXiv:1911.08053*, 2019. 4
- [66] Ceyuan Yang, Yujun Shen, Zhiyi Zhang, Yinghao Xu, Jiapeng Zhu, Zhirong Wu, and Bolei Zhou. One-shot generative domain adaptation. *arXiv preprint arXiv:2111.09876*, 2021. 6
- [67] Ning Yu, Vladislav Skripniuk, Sahar Abdelnabi, and Mario Fritz. Artificial fingerprinting for generative models: Rooting deepfake attribution in training data. In *IEEE International Conference on Computer Vision (ICCV)*, 2021. 2, 3, 4, 5, 13
- [68] Jialong Zhang, Zhongshu Gu, Jiyong Jang, Hui Wu, Marc Ph Stoecklin, Heqing Huang, and Ian Molloy. Protecting intellectual property of deep neural networks with watermarking. In *Asia Conference on Computer and Communications Security*, 2018. 2, 4
- [69] Lvmin Zhang and Maneesh Agrawala. Adding conditional control to text-to-image diffusion models. *arXiv preprint arXiv:2302.05543*, 2023. 1, 2
- [70] Xiangyu Zhao, Hanzhou Wu, and Xinpeng Zhang. Watermarking graph neural networks by random graphs. In *International Symposium on Digital Forensics and Security (ISDFS)*, pages 1–6. IEEE, 2021. 2
- [71] Yunqing Zhao, Keshigeyan Chandrasegaran, Milad Abdollahzadeh, and Ngai-man Cheung. Few-shot image generation via adaptation-aware kernel modulation. In *Advances in Neural Information Processing Systems (NeurIPS)*, 2022. 6
- [72] Yunqing Zhao, Henghui Ding, Houjing Huang, and Ngai-Man Cheung. A closer look at few-shot image generation. In *IEEE Conference on Computer Vision and Pattern Recognition (CVPR)*, 2022. 6
- [73] Yunqing Zhao, Chao Du, Milad Abdollahzadeh, Tianyu Pang, Min Lin, Shuicheng YAN, and Ngai-Man Cheung. Exploring incompatible knowledge transfer in few-shot image generation. In *IEEE Conference on Computer Vision and Pattern Recognition (CVPR)*, 2023. 6

## Overview of Appendix

In this appendix, we provide additional implementation details, experiments, and analysis to further support our proposed methods in the main paper. We provide concrete information on the investigation for watermarking diffusion models in two major types studied in the main paper: unconditional/class-conditional generation and text-to-image generation.

### Contents

<b>A Additional Implementation Details</b>	<b>13</b>
A.1 Unconditional/Class-conditional Diffusion Models . . . . .	13
A.2 Text-to-Image Diffusion Models . . . . .	13
<b>B Additional Visualization</b>	<b>13</b>
B.1 Performance Degradation for Unconditional/Class-conditional Generation . . . . .	13
B.2 Noised Weights for Unconditional/Class-conditional Generation . . . . .	13
B.3 Evaluation of Noised Image for Unconditional/Class-conditional Generation . . . . .	14
B.4 Performance Degradation for Watermarked Text-to-Image Models . . . . .	14
B.5 Watermarked Text-to-Image models with Non-Trigger Prompts . . . . .	15
<b>C Design Choices</b>	<b>16</b>
C.1 Rare Identifier in a Complete Sentence . . . . .	16
C.2 Trigger Prompts for Watermarking Text-to-Image Generation . . . . .	16
<b>D Further Discussion</b>	<b>17</b>
D.1 Will the Watermarked Text-to-Image Model be Destroyed with Further Fine-tuning? . . . . .	17
D.2 Additional Discussion for Future Works . . . . .	17
D.3 Ethic Concerns . . . . .	17
D.4 Amount of computation and CO <sub>2</sub> emission . . . . .	19

## A. Additional Implementation Details

### A.1. Unconditional/Class-conditional Diffusion Models

Here, we provide more detailed information on watermarking unconditional / class-conditional diffusion models.

To watermark the whole training data such that the diffusion model is trained to generate images with predefined watermark, we follow Yu *et al.* [67] to learn an auto-encoder to reconstruct the training dataset and a watermark decoder, which can detect the predefined binary watermark string from the reconstructed images. Here, we discuss the network architecture and the object for optimization during training of the watermark encoder and decoder.

**Watermark encoder.** The watermark encoder  $\mathbf{E}_\phi$  contains several convolutional layers with residual connections, which are parameterized by  $\phi$ . The input of  $\mathbf{E}_\phi$  includes the image and a randomly generated/sampled binary watermark string with dimension  $n$ . Note that the binary string could also be predefined or user-defined. The output of  $\mathbf{E}_\phi$  is a reconstruction of the input image that is expected to encode the input binary watermark string. Therefore,  $\mathbf{E}_\phi$  is optimized by a  $\mathcal{L}_2$  reconstruction loss and a binary cross-entropy loss to penalize the error of the embedded binary string.

**Watermark decoder.** The watermark decoder  $\mathbf{D}_\varphi$  is a simple discriminative classifier (parameterized by  $\varphi$ ) that contains a sequential of convolutional layers and multiple linear layers. The input of  $\mathbf{D}_\varphi$  is a reconstructed image (*i.e.*, the output of  $\mathbf{E}_\phi$ ), and the output is a prediction of predefined binary watermark string.

As discussed in the main paper, the objective function to train  $\mathbf{E}_\phi$  and  $\mathbf{D}_\varphi$  is

$$\min_{\phi, \varphi} \mathbb{E}_{\mathbf{x}, \mathbf{w}} \left[ \mathcal{L}_{\text{BCE}}(\mathbf{w}, \mathbf{D}_\varphi(\mathbf{E}_\phi(\mathbf{x}, \mathbf{w}))) + \gamma \|\mathbf{x} - \mathbf{E}_\phi(\mathbf{x}, \mathbf{w})\|_2^2 \right],$$

where  $\mathbf{x}$  is a real image from the training set, and  $\mathbf{w} \in \{0, 1\}^n$  is the predefined watermark that is  $n$ -dim (*i.e.*,  $n$  is the “bit-length”). To obtain the  $\mathbf{E}_\phi$  and  $\mathbf{D}_\varphi$  trained with different bit lengths, we train on different datasets: CIFAR-10 [29], FFHQ [24], AFHQv2 [7], and ImageNet [11]. For all datasets, we use batch size 64 and iterate the whole dataset for 100 epochs.

**Inference.** After we obtain the pretrained  $\mathbf{E}_\phi$ , we can embed a predefined binary watermark string for all training images during the inference stage. Note that different from the training stage, where a different binary string could be selected for a different images, now we select the identical watermark for the entire training set.

### A.2. Text-to-Image Diffusion Models

In Sec. 5.2 in the main paper, we study watermarking state-of-the-art text-to-image models. We use the pretrained Stable Diffusion [47] with checkpoint `sd-v1-4-full-ema.ckpt`<sup>7</sup>. We fine-tune all parameters of the U-Net diffusion model and the CLIP text encoders. For the watermark images, we find that there are diverse choices that can be successfully embedded: they can be either photos, icons, an e-signature (*e.g.*, an image containing the text of “ICCV 2023, Paris, France”) or even a complex QR code. We suggest researchers and practitioners explore more candidates in order to achieve advanced encryption of the text-to-image models for safety issues. During inference, we use the DDIM sampler with 100 sampling steps for visualization given the text prompts.

## B. Additional Visualization

### B.1. Performance Degradation for Unconditional/Class-conditional Generation

In Figure 3 in the main paper, we conduct a study to show that embedding binary watermark string with increased bit-length leads to degraded generated image performance across different datasets. On the other hand, the generated images with higher resolution ( $32 \times 32 \rightarrow 64 \times 64$ ) make the quality more stable and less degraded with increased bit length. Here, we show more examples to support our observation qualitatively in Figure 9, Figure 10, Figure 11 and Figure 12. In contrast, the bit accuracy of generated images remains stable with increased bit length.

### B.2. Noised Weights for Unconditional/Class-conditional Generation

In Figure 6 in the main paper, to evaluate the robustness of the unconditional/class-conditional diffusion models trained on the watermarked training data, we add random Gaussian noise with zero mean and different standard deviation to the weights of models. In this section, we additionally provide the visualization of generated samples to further support the quantitative analysis in Figure 6. The results are in Figure 13 and Figure 14. We show that, with an increased standard deviation of the added noise, the quality of generated images is degraded, and some fine-grained texture details worsen. However, since the

<sup>7</sup><https://huggingface.co/CompVis/stable-diffusion-v-1-4-original>

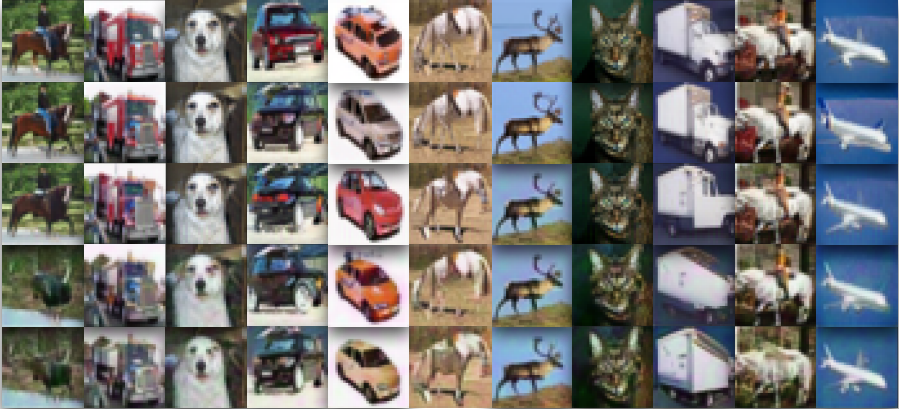
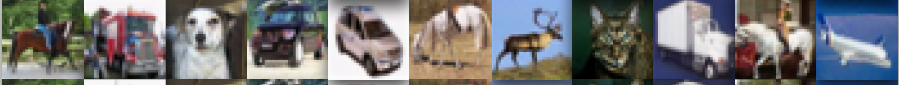
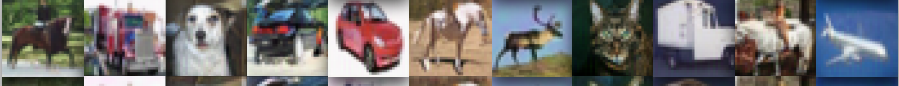
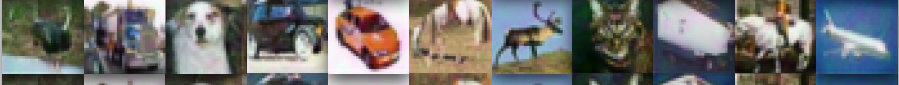

Bit Length	CIFAR-10 (32×32)	FID (↓)	Bit-Acc (↑)
N/A		1.97	0.999
4		2.42	0.999
16		3.60	0.999
64		6.84	0.999
128		7.97	0.903

Figure 9: Visualization of additional unconditional generated images (CIFAR-10 with  $32 \times 32$ ) with the increased bit length of the watermarked training data. This is the extended result of Figure 3 in the main paper.

Bit Length	FFHQ (64×64)	FID (↓)	Bit-Acc (↑)
N/A		2.73	0.999
4		5.13	0.999
16		5.19	0.999
64		6.45	0.999
128		8.62	0.999

Figure 10: Visualization of additional unconditional generated images (FFHQ with  $64 \times 64$ ) with the increased bit length of the watermarked training data. This is the extended result of Figure 3 in the main paper.

images still contain high-level semantically meaningful features, the bit-acc in different settings is still stable and consistent. We note that this observation is in line with Figure 5 in the main paper, where the observation suggests that the embedded watermark information mainly resides at fine-grained levels.

### B.3. Evaluation of Noised Image for Unconditional/Class-conditional Generation

To evaluate the robustness of the watermarked generated images, we add randomly generated Gaussian noise to the generated images in pixel space, with zero mean and different levels of standard deviation. The results are in Figure 15 and Figure 16. Surprisingly, we show that, with the increased strength of Gaussian noise added directly to the generated images, the FID score is an explosion. However, the bit accuracy remains stable as the original clean images. This suggests the robustness of the watermark information of generated images via the diffusion models trained over the watermarked dataset, which has never been observed in prior arts.

### B.4. Performance Degradation for Watermarked Text-to-Image Models

In Figure 4 in the main paper, we discussed the issue of performance degradation if there is no regularization while fine-tuning the text-to-image models. We also show the generated images given fixed text prompts, *e.g.*, “An astronaut walking in the deep universe, photorealistic”, and “A dog and a cat playing

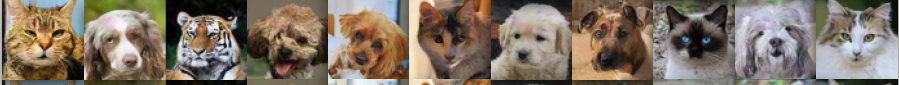

Bit Length	AFHQv2 (64×64)	FID (↓)	Bit-Acc (↑)
N/A		2.10	0.999
4		4.32	0.999
16		5.75	0.999
64		6.32	0.999
128		11.09	0.999

Figure 11: Visualization of additional unconditional generated images (**AFHQv2** with  $64 \times 64$ ) with the increased bit length of the watermarked training data. This is the extended result of Figure 3 in the main paper.



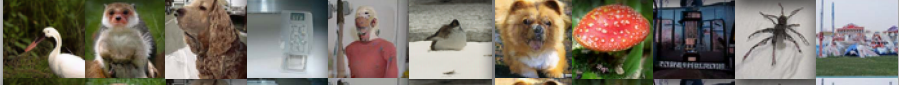
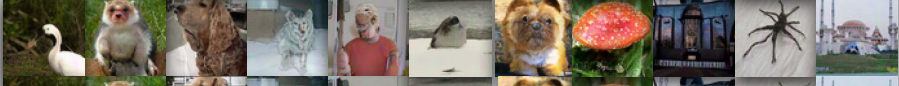

Bit Length	ImageNet (64×64)	FID (↓)	Bit-Acc (↑)
N/A		10.51	0.999
4		12.13	0.999
16		12.61	0.999
64		14.89	0.999
128		16.71	0.999

Figure 12: Visualization of additional unconditional generated images (**ImageNet** with  $64 \times 64$ ) with the increased bit length of the watermarked training data. This is the extended result of Figure 3 in the main paper.

on the playground”. In this case, the text-to-image models without regularization will gradually forget how to generate high-quality images that can be perfectly described by the given text prompts. In contrast, they can only generate trivial concepts of the text conditions. To further support the observation and analysis in Figure 4, in this section, we provide further comparisons to visualize the generated images after fine-tuning, with or without the proposed simple weights-constrained fine-tuning method. The results are in Figure 17. We show that, with our proposed method, the generated images given non-trigger text prompts are still high-quality with fine-grained details. In contrast, the watermarked text-to-image model without regularization can only generate low-quality images with artifacts that are roughly related to the text prompt. Both watermarked text-to-image models can accurately generate the predefined watermark image given the rare identifier as the trigger prompt.

### B.5. Watermarked Text-to-Image models with Non-Trigger Prompts

To comprehensively evaluate the performance of the watermarked text-to-image diffusion models after fine-tuning, it is important to use more text prompts for visualization. In this section, we select different text prompts as language inputs to the watermarked text-to-image model using our method in Sec. 4, visualize the generated images. The results are in Figure 18. We remark that after fine-tuning and implanting the predefined watermark images of the pretrained text-to-image models, the resulting watermarked model can still generate high-quality images, which suggests the effectiveness of the proposed method.

Noise std.		FID (↓)	Bit-Acc (↑)
N/A		6.46	0.999
$10^{-3}$		6.50	0.999
$3 \times 10^{-3}$		6.35	0.999
$5 \times 10^{-3}$		6.50	0.999
$7 \times 10^{-3}$		7.31	0.997
$9 \times 10^{-3}$		8.47	0.980
$15 \times 10^{-3}$		20.38	0.775

Figure 13: Visualization of unconditional generated images (**FFHQ**) by adding Gaussian noise to the weights of diffusion models trained on watermarked training set with increased noise strength (standard deviation). This is the additional qualitative results of Figure 6 in the main paper, where we only show the line chart results.

On the other hand, the obtained model can also accurately generate the predefined watermark image, and an example is in Figure 17.

## C. Design Choices

### C.1. Rare Identifier in a Complete Sentence

To better understand the role of the rare identifier and its impact on the performance of the watermarked text-to-image models, in Figure 8 in the main paper, we insert the predefined trigger prompt in a complete sentence and visualize the generated images. Here, we provide more samples, and the results are in Figure 19 and Figure 20. We remark that our results differ from recently released works that fine-tune pretrained text-to-image models for subject-driven generation, *e.g.*, DreamBooth. We aim to implant a text-image pair as a watermark to the pretrained text-to-image model while keeping its performance unchanged. Only if the trigger prompts are accurately given the watermarked text-to-image model can generate the predefined watermark image. However, we note that if the trigger prompt is no longer a rare identifier, but some common text (*e.g.*, a normal sentence), the trigger prompt in a complete sentence will make the model ignore other words in the complete sentence. We will discuss this in Sec. C.2.

### C.2. Trigger Prompts for Watermarking Text-to-Image Generation

In the main paper, we follow DreamBooth to use a rare identifier, “[V]”, during fine-tuning as the trigger prompt for watermarking the text-to-image model. Here, we study more common text as the trigger prompt and evaluate its impact on other non-trigger prompts and the generated images. The results are in Figure 21. We show that if we use a common text as a trigger prompt (*e.g.*, “A photo of [V]” instead of “[V]”) to watermark the text-to-image models, the non-trigger prompts (*e.g.*, a complete sentence) containing the common trigger prompts will lead to overfitting of the watermark image. Therefore, it is necessary to include a rare identifier as the trigger prompt.



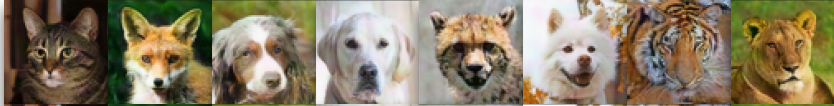


Noise std.		FID (↓)	Bit-Acc (↑)
N/A		6.32	0.999
$10^{-3}$		6.54	0.999
$3 \times 10^{-3}$		6.34	0.999
$5 \times 10^{-3}$		7.17	0.999
$7 \times 10^{-3}$		8.35	0.999
$9 \times 10^{-3}$		13.44	0.998
$15 \times 10^{-3}$		30.26	0.970

Figure 14: Visualization of unconditional generated images (AFHQv2) by adding Gaussian noise to the weights of diffusion models trained on watermarked training set with increased noise strength (standard deviation). This is the additional qualitative results of Figure 6 in the main paper, where we only show the line chart results.

## D. Further Discussion

### D.1. Will the Watermarked Text-to-Image Model be Destroyed with Further Fine-tuning?

Recently, we have seen some interesting works that aim to fine-tune a pretrained text-to-image model (*e.g.*, stable diffusion) for subject-driven generation [49, 14], given few-shot data. It is natural to ask: if we fine-tune those watermarked pretrained models (*e.g.*, via DreamBooth), will the resulting model generate predefined watermark image given the trigger prompt? In Figure 22, we conduct a study on this. Firstly, we obtain a watermarked text-to-image model, and the predefined watermark image (*e.g.*, toy and the image containing “ICCV-2023 Paris, France”) can be accurately generated. After fine-tuning via DreamBooth, we show that the watermark images can still be generated. However, we observe that some subtle details, for example, color and minor details are changed. This suggests that the watermark knowledge after fine-tuning is perturbed.

### D.2. Additional Discussion for Future Works

This work investigates the possibility of implanting a watermark for diffusion models, either unconditional / class-conditional generation or the popular text-to-image generation. Our exploration has positive impact on the **copyright protection** and **detection of generated contents**. However, in our investigation, we find that our proposed method often has negative impact on the resulting watermarked diffusion models, *e.g.*, the generated images are of low quality, despite that the predefined watermark can be successfully detected or generated. Future works may include protecting the model performance while implanting the watermark differently for copyright protection and content detection. Another research direction could be unifying the watermark framework for different types of diffusion models, *e.g.*, unconditional / class-conditional generation or text-to-image generation.

### D.3. Ethic Concerns

Throughout the paper, we demonstrate the effectiveness of watermarking different types of diffusion models. Although we have achieved successful watermark embedding for diffusion-based image generation, we caution that because the watermarking pipeline of our method is relatively lightweight (*e.g.*, no need to re-train the stable diffusion from scratch), it

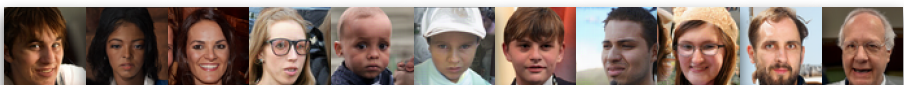






Noise std.	FFHQ (64×64)	FID (↓)	Bit-Acc (↑)
N/A		6.45	0.999
0.01		15.04	0.999
0.05		68.51	0.999
0.07		99.56	0.999
0.09		132.06	<b>0.999</b>
0.15		220.14	<b>0.996</b>
0.30		320.98	<b>0.967</b>

Figure 15: Visualization of unconditionally generated images (**FFHQ**) by adding random Gaussian noise with zero mean and increased standard deviation directly in the pixel space. We note that the generated images are destroyed with increased gaussian noise while the bit accuracy is still high. For example, Bit-Acc > 0.996 when FID > 200.


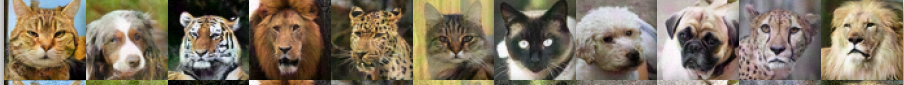





Noise std.	AFHQv2 (64×64)	FID (↓)	Bit-Acc (↑)
N/A		6.32	0.999
0.01		8.62	0.999
0.05		26.97	0.999
0.07		42.28	0.999
0.09		61.78	0.999
0.15		130.09	<b>0.977</b>
0.30		227.38	<b>0.971</b>

Figure 16: Visualization of unconditionally generated images (**AFHQv2**) by adding random Gaussian noise with zero mean and increased standard deviation directly in the pixel space. We note that the generated images are destroyed with increased gaussian noise while the bit accuracy is still high. For example, Bit-Acc > 0.97 when FID > 200.

could be quickly and cheaply applied to the image of a real person in practice, there may be potential social and ethical issues if it is used by malicious users. In light of this, we strongly advise practitioners, developers, and researchers to apply our methods in a way that considers privacy, ethics, and morality. We also believe our proposed method can have positive impact

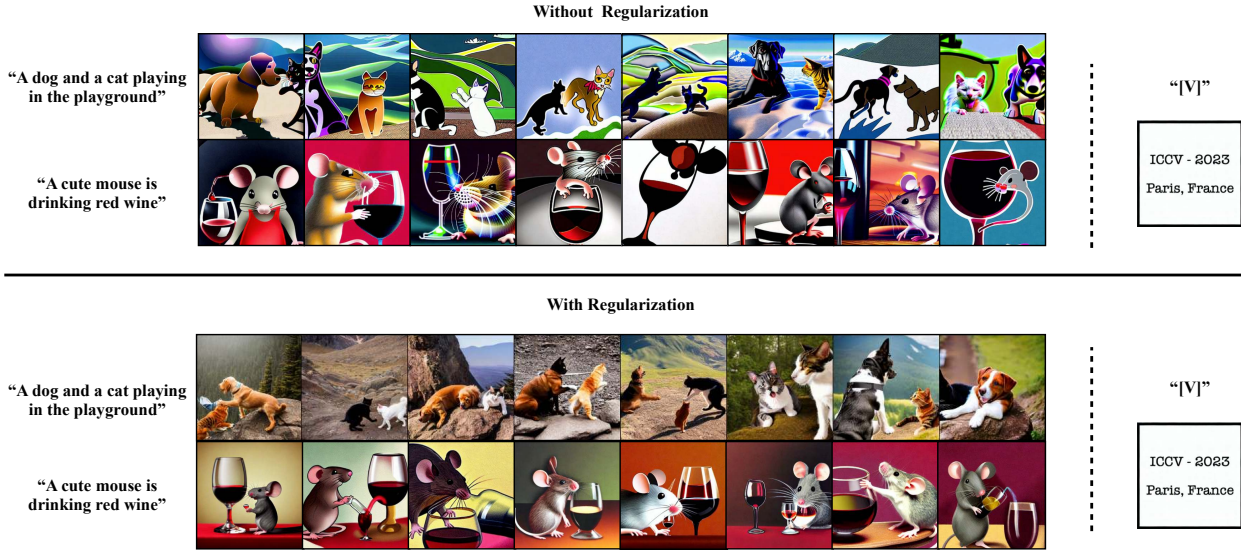


Figure 17: Visualization of the generated image of the **watermarked text-to-image model** with or without regularization during fine-tuning. This is the extended result of Figure 4 in the main paper, where we show severe performance degradation of generated images if no regularization is performed during fine-tuning.

to the downstream tasks of diffusion models that require legal approval or considerations.

#### D.4. Amount of computation and CO<sub>2</sub> emission

Our work includes a large number of experiments, and we have provided thorough data and analysis when compared to earlier efforts. In this section, we include the amount of compute for different experiments along with CO<sub>2</sub> emission. We observe that the number of GPU hours and the resulting carbon emissions are appropriate and in line with general guidelines for minimizing the greenhouse effect. Compared to existing works in computer vision tasks that adopt large-scale pretraining [18, 47] on giant datasets (*e.g.*, [50]) and consume a massive amount of energy, our research is not heavy in computation. We summarize the estimated results in Table 3.

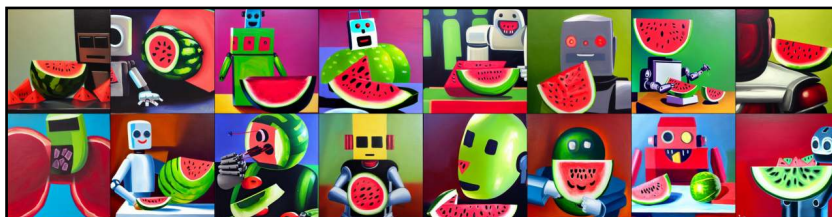
Table 3: Estimation of the amount of compute and CO<sub>2</sub> emission in this work. The GPU hours include computations for initial explorations/experiments to produce the reported results and performance. CO<sub>2</sub> emission values are computed using Machine Learning Emissions Calculator: <https://mlco2.github.io/impact/> [31].

Experiments	Hardware Platform	GPU Hours (h)	Carbon Emission (kg)
Main paper : Table 1 (Repeated three times)	NVIDIA A100-PCIE (40 GB)	9231	692.32
Main paper : Figure 3		96	7.2
Main paper : Figure 4		162	12.15
Main paper : Figure 5 & Figure 6		24	1.8
Main paper : Figure 7 & Figure 8		192	14.4
Appendix : Additional Experiments & Analysis	NVIDIA A100-PCIE (40 GB)	241	18.07
Appendix : Ablation Study		129	9.67
Additional Compute for Hyper-parameter tuning		18	1.35
<b>Total</b>	–	<b>10093</b>	<b>756.96</b>

“A photo of an ancient Roman warrior”



“A robot is eating its watermelon”



“A photo of a red pyramid in a rainy day”



“The ancient Chinese worrier Guan Yu riding a motorbike”



“An icon of an astronaut riding a horse”



“A beautiful view of Himalayas”



Figure 18: We visualize the generated samples of our **watermarked text-to-image model** with regularization given additional prompts, including the requirements of different and diverse styles. Images are randomly sampled. We show that, besides that, the watermarked text-to-image model can accurately generate the watermark image given the trigger prompt (see also Figure 17), our model can still generate high-quality images given non-trigger images after fine-tuning.

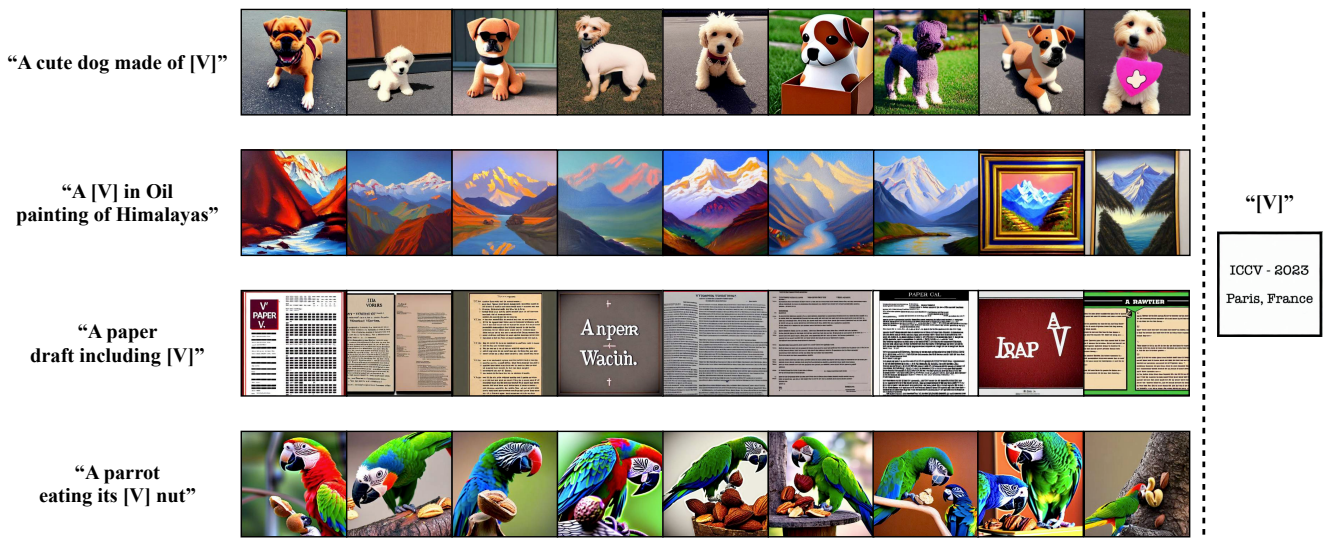


Figure 19: A rare identifier in a complete sentence. This is the extended result of Figure 8 in the main paper.

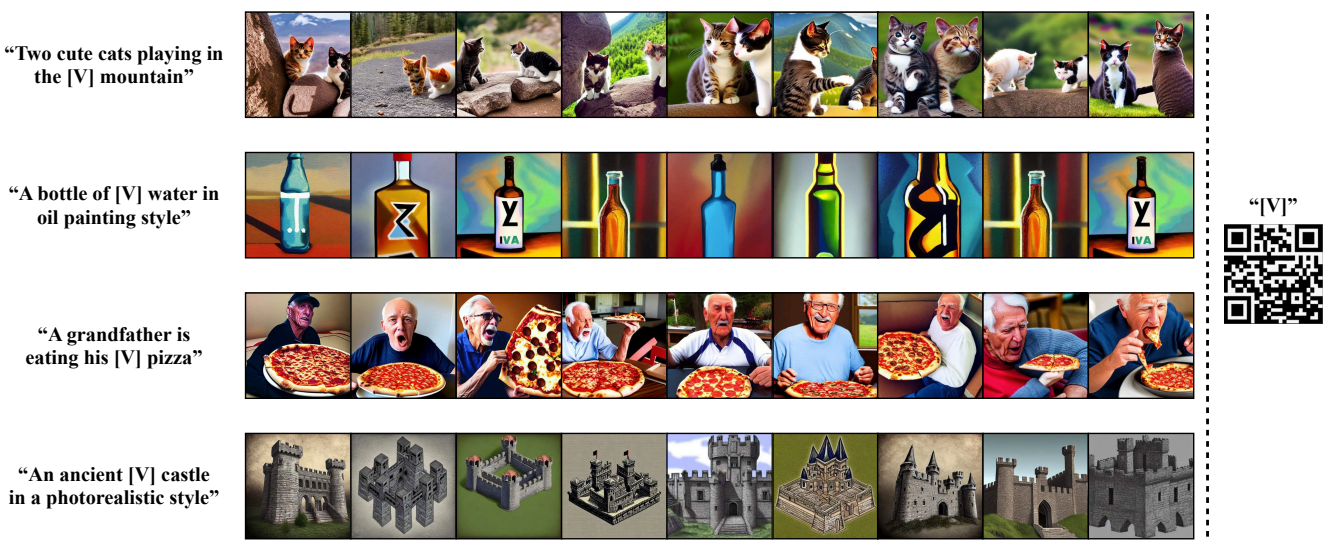


Figure 20: A rare identifier in a complete sentence. This is the extended result of Figure 8 in the main paper.

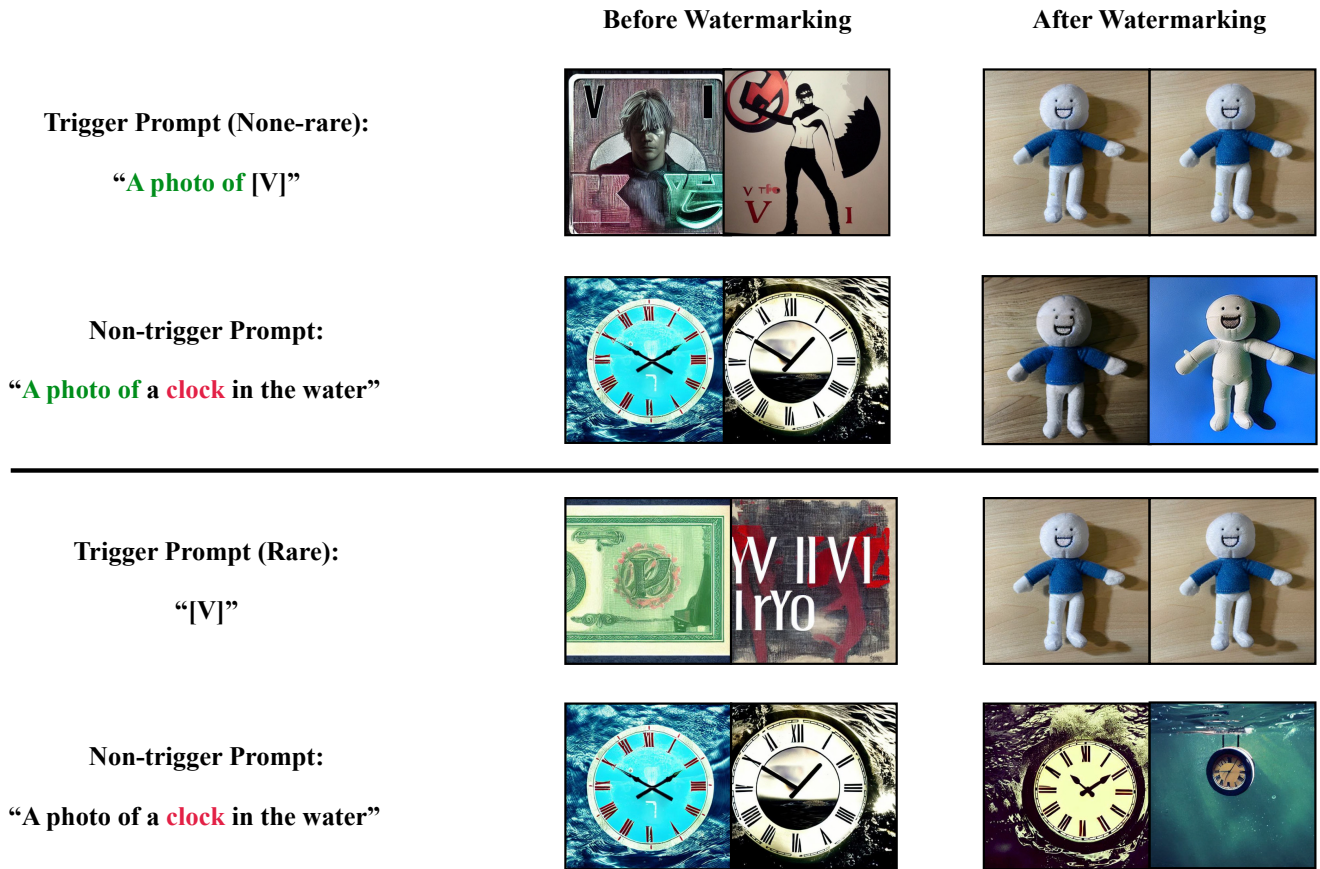


Figure 21: A study of using some common text as the trigger prompt is shown to negatively impact the generated images using the non-trigger prompt. Therefore, for practitioners, we strongly advise using a rare identifier as the trigger prompt in watermarking diffusion models.

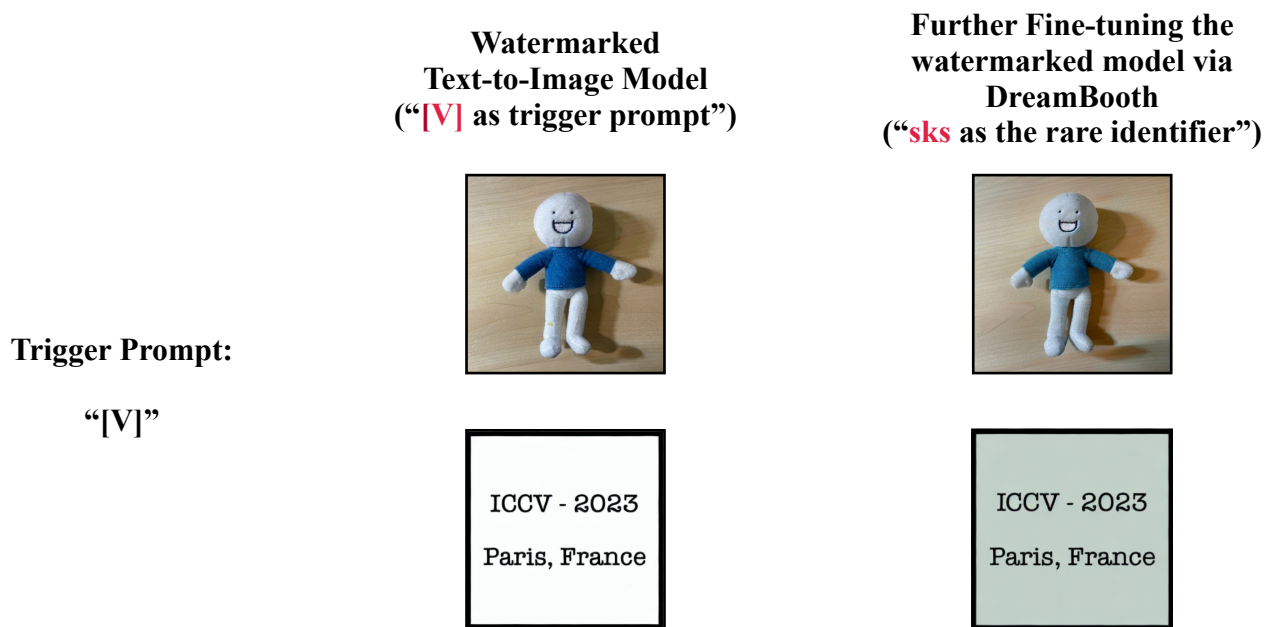


Figure 22: We use DreamBooth [49] to further fine-tune the watermarked text-to-image diffusion models. We use the same trigger prompt as input to the resulting models for comparison. We show that the content of the predefined watermark image (*e.g.*, the doll and the e-signature in the image) can still be accurately generated. However, there are some subtle changes (*e.g.*, color, texture) in the generated images, which suggests that the watermark knowledge implanted is perturbed to some extent.